Polymorphic Transition in Disordered Poly(L-lactide) Crystals Induced by Annealing at Elevated Temperatures

Pengju Pan, Bo Zhu, Weihua Kai, Tungalag Dong, and Yoshio Inoue*

Department of Biomolecular Engineering, Tokyo Institute of Technology, 4259-B-55 Nagatsuta, Midori-ku, Yokohama 226-8501, Japan

Received February 15, 2008; Revised Manuscript Received March 27, 2008

ABSTRACT: Effects of annealing conditions and molecular weight (MW) on the crystalline phase transition in poly(L-lactide) (PLLA) were studied by wide-angle X-ray diffraction (WAXD), Fourier transform infrared (FTIR) spectroscopy, and differential scanning calorimetry (DSC). The disordered crystal (α′-form) of PLLA was found to transform into the α one during annealing process at elevated temperatures. The α′-to-α transition is quite dependent on the annealing period (t_a: 0−1440 min) and annealing temperature (T_a: 120−160 °C). With increasing T_a, the polymorphic transition progresses much more rapidly. The α′-to-α transition is mainly involved by the slight rearrangement of the chain conformation (especially related to the side groups) and packing manner in the unit cell to the more energy-favorable state, corresponding to the reduction of unit cell dimension. Besides, it was proposed that the α′-to-α transformation mainly proceeds by the direct solid−solid transition mechanism. Moreover, it was found that MW affects the crystalline phase transition significantly. In the low-MW PLLA sample, the α′-to-α transition becomes much faster, and it can proceed prominently even when annealed at relatively lower temperature.

Introduction

Poly(L-lactide) (PLLA), as a biodegradable polymer, has attracted considerable interest from both fundamental and practical perspectives because it can be synthesized from renewable resources and is thus environmentally and economically appropriate. Since its degradation products are nontoxic and bioresorbable, this polymer is one of the selected few candidates for use in biomedical fields, such as implant materials, surgical suture, and controlled drug delivery systems.[1] Furthermore, the attributes of biodegradability, producibility from renewable resources, good mechanical properties, and versatile fabrication processes make it a promising material for many disposable products, such as baby diapers and plastic bags, as well as for traditional applications where common thermoplastics are employed, for instance, industrial devices, packaging film, and fiber materials.[1]

PLLA can crystallize in α-, *β*-, or *γ*-forms, depending on the processing conditions.[2–4] The most common and stable polymorph, α-form, with a 10_3 helical chain conformation where two chains are interacting in an orthorhombic unit cell, can be developed from the melt or solution under normal conditions.[2] The *β*-crystal was produced by stretching the α-form at high drawing ratio and high temperature.[3] The *γ*-form was obtained by epitaxial growth on the hexamethylbenzene substrate.[4] Recently, a new disordered form, named as α′-form, was proposed for the PLLA sample crystallized at lower temperature.[5]

As for the polymorphic polymers, a broad range of properties, for instance, thermal, mechanical, and optical properties, greatly depend on the crystalline structure as well as morphology.[6] Besides, in the case of biodegradable polymers, their biodegradability is also influenced by the crystal modifications.[7] Therefore, regulating the crystalline structure and morphology is an important issue in polymer processing because of its ability to tailor the properties of final products. From this point of view, studies on the polymorphic crystallization and the phase behavior of the different polymorphs are of fundamental importance. The polymorphism, as well as the polymorphic crystallization and phase behavior of the traditional semicrystalline thermoplastics, for example, polypropylene, polystyrene, and etc., have been extensively investigated in the recent decades.[8–10]

At present, the crystallization kinetics of PLLA as well as the crystalline structure of α-form PLLA have been widely studied.[2,11–13] As we know, PLLA is usually molded at 100−120 °C in the industrial melt processing because of the higher crystallization rate. It has been reported that when crystallized at this temperature region (100−120 °C), the mixture of α′- and α-form crystals is formed.[5a–d] This result indicates that the α′-crystals indeed exist widely in the PLLA-based products. Therefore, study on the structure and properties of the α′-crystal is highly important from the perspective of practical application. So far, it has been proposed that the slightly structural difference between the α′- and α-crystals is concerning the chain conformation and packing mode,[5] but almost no detailed and quantitative result about this structural difference was reported. As for the disordered-type α′-form, its wide-angle X-ray diffraction (WAXD) patterns and vibrational spectra have been addressed.[5] Because of the high similarity between the WAXD patterns and Fourier transform infrared (FTIR) spectra of the α′- and α-crystals, the detailed structure and morphology as well as the reason for the formation of the α′-crystal has not yet been well explained.

Very recently, on the basis of time-resolved measurements of FTIR spectra and WAXD patterns, it was found that during the heating process the α′-crystal transforms into the α one before melting, which corresponds to a small exotherm in the DSC thermogram prior to the dominant melting peak.[5a,c,d] However, as we know, the time and temperature, both of which are key factors for the phase transition process, change simultaneously in the heating scan. Accordingly, several processes, including the phase transition, melting, and recrystallization, are usually overlapped severely upon heating. As a result, the features related to the phase transition process cannot be clearly observed during the heating process.[8b] Contrarily, in the isothermal annealing process at elevated temperature, the conditions for phase transition can be well controlled by

* To whom corresponding should be addressed: Tel +81-45-924-5794; Fax +81-45-924-5827; e-mail inoue.y.af@m.titech.ac.jp.

10.1021/ma800343g CCC: $40.75
Published on Web 05/22/2008

Table 1. Molecular Weight and Thermal Properties of PLLA Samples

code	M_n (kg/mol)	M_w (kg/mol)	M_w/M_n	T_g (°C)	T_m^0 (°C)
PLLA15	15.4	21.3	1.38	48.0	174.2
PLLA118	118.3	176.6	1.49	59.1	192.4

changing the annealing period (t_a) and annealing temperature (T_a). This makes it possible to more distinctly detect the transformation kinetics and the structural changes during the phase transition process and also to find the favorite condition for the transition process.[8d,9a,14] Therefore, it is considered that the annealing method, especially at elevated temperature, is possibly more efficient for studying the phase behavior of the PLLA α′- and α-crystals.

FTIR is highly sensitive to the chain conformation and packing manner, making it widely useful in the studies of crystallization, melting, and phase transition behavior of polymers.[9,12a,b,13] For the polymorphic polymers, the characteristic FTIR bands can be correlated to the different crystal modifications and typically stay distinguishable in a certain process. This makes it possible to illustrate the mechanism for a polymorphic transition process from the molecular level. Therefore, FTIR spectroscopy was employed in the present study in combination with the WAXD and DSC analysis.

On the other hand, the molecular weight (MW) usually plays an important role in the crystallization, melting, and polymorphism of polymers.[15] Our previous paper has reported that the crystallization kinetics and melting behavior of PLLA are dependent on its MW considerably.[5a] Therefore, study on the MW effects on the polymorphic transition is also significant for better understanding the structure and phase behavior of the α′- and α-crystals.

In this work, the structural changes for the PLLA α′-crystal during annealing process at elevated temperatures (T_a = 120−160 °C) were investigated by WAXD and FTIR in detail. The annealing-induced α′-to-α transition was confirmed. The effects of annealing period (t_a), annealing temperature (T_a), and MW on the α′-to-α phase transition process were studied. The melting behavior of PLLA after the annealing-induced phase transition was also analyzed by DSC. Besides, the mechanism for the polymorphic transition process was discussed on the basis of FTIR spectra.

Experimental Section

Materials. PLLA samples were attained from Unitika Co. Ltd. (Kyoto, Japan). The number-average molecular weight (M_n), weight-average molecular weight (M_w), and M_w/M_n for these two types of samples were tabulated in Table 1. Before use, the samples were purified by precipitating into ethanol from chloroform solution and then were dried in the vacuum oven at 40 °C for 3 days. The glass transition temperature (T_g) and equilibrium melting point (T_m^0) of the PLLA samples, which are shown in Table 1, were evaluated according to the procedures reported previously.[5a]

Preparation of PLLA α′- and α-Crystals. For both the two samples, the α′-form crystals were prepared by the isothermal melt-crystallization at 80 °C for 3 h after melting at 200 °C for 2 min. In all the annealing experiments for WAXD, FTIR, and DSC analysis, the same thermal procedure was maintained. For comparison, the normal α-crystals of PLLA118 and PLLA15 were also prepared by melt-crystallization at 150 °C for 12 h and at 140 °C for 6 h, respectively, after melting at 200 °C for 2 min. WAXD and FTIR results show that the α′- and α-crystals were successfully developed in the corresponding processes.

Measurements. Wide-Angle X-ray Diffraction (WAXD). WAXD analysis was performed on a Rigaku RU-200 (Rigaku Co., Tokyo, Japan) with Ni-filtered Cu Kα radiation (λ = 0.154 18 nm). PLLA sample was hot-pressed at 200 °C with a pressure of 10 MPa after melting at this temperature for 2 min. Subsequently, it was transferred to a vacuum oven preset at 80 °C and held for 3 h for the isothermal crystallization. Then, the sample was heated to the elevated temperature (T_a = 120−160 °C) and annealed isothermally for different periods (t_as). Finally, the annealed sample was analyzed by WAXD at room conditions. All the measurements were operated at 40 kV and 200 mA from 5° to 45° at a 2θ scan rate of 1°/min.

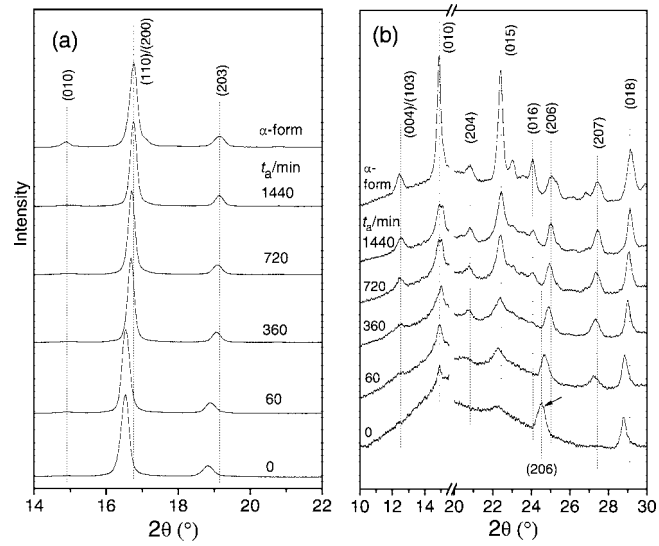

Figure 1. (a) WAXD patterns and (b) enlarged patterns of the normal PLLA118 α-crystal unannealed and annealed (at 150 °C for the indicated periods (t_a/min)) PLLA118 α′-crystals.

Fourier Transform Infrared (FTIR) Spectroscopy. FTIR measurements were performed on an FTIR-6100 spectrometer (JASCO, Tokyo, Japan) equipped with an IMV-4000 multichannel infrared microscope (JASCO, Tokyo, Japan) and a MCT detector in the transmission mode. PLLA sample was placed between two pieces of BaF_2 slides, and then it was melted at 200 °C for 2 min in a LK-600FTIR hot stage (Linkam Scientific Instruments Ltd., Surrey, UK) equipped with a cooling unit (L600A) under the protection of the dry nitrogen gas. Afterward, the sample was cooled to 80 °C at a rate of 100 °C/min by a flow of liquid nitrogen. After crystallized for 3 h, it was heated to the higher temperature (T_a = 120−160 °C) and annealed isothermally for different periods (t_as). Finally, it was cooled to 23 ± 1 °C for FTIR measurement. All the spectra were collected with 64 scans and a resolution of 2 cm^{-1}.

Differential Scanning Calorimetry (DSC). DSC measurements were carried out on a Pyris Diamond DSC instrument (Perkin-Elmer Japan Co., Yokohama, Japan) equipped with an intracooler 2P cooling accessory. The temperature and heat flow at different heating rates were calibrated by an indium standard under the nitrogen purging. PLLA sample (6−8 mg) was weighed and sealed in an aluminum pan. First, the sample was crystallized isothermally at 80 °C for 3 h after melted at 200 °C for 2 min. Then, it was heated to the higher temperature (T_a = 120−160 °C) at 100 °C/min and annealed for different periods (t_as). Finally, the sample was heated to 200 at 10 °C/min to observe the melting behavior. Because it is impractical to use the DSC as an oven for longer annealing times, only the samples annealed for $t_a \leq 360$ min were examined here.

Gel Permeation Chromatography (GPC). Molecular weight of the PLLA samples was measured on TOSOH HLC-8220 GPC system assembled with a VISCOTEK T-60AV viscometer. Chloroform was used as the eluent at a flow rate of 1.0 mL/min. TOSOH TSK standard polystyrene samples with the narrow molecular weight distribution were used as standards to calibrate the GPC elution curve. After the annealing process, the molecular weight (MW) of the sample was also checked by GPC. No discernible change in MW of the PLLA118 sample was observed after annealing at 160 °C for 6 and 24 h, and also their weights are nearly

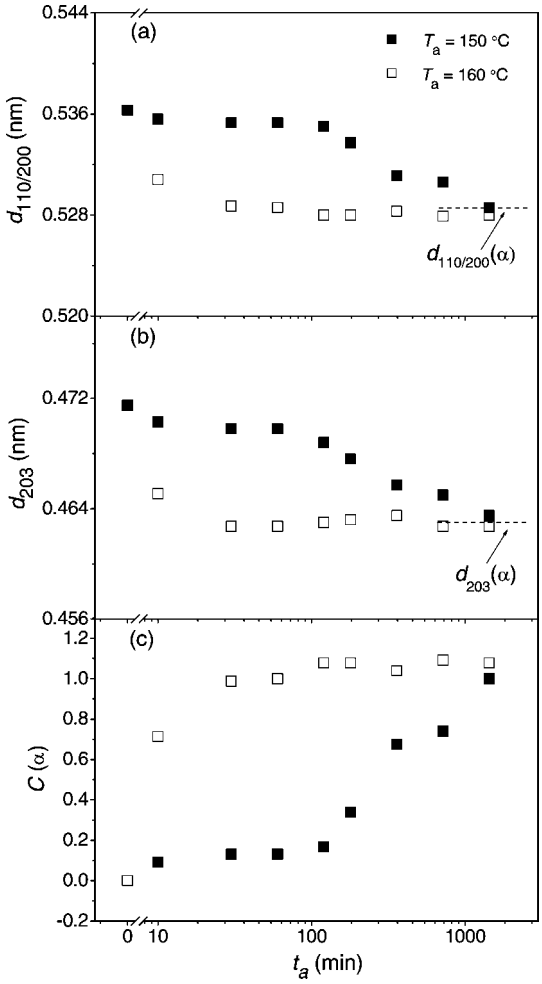

Figure 2. Lattice spacings estimated from (a) (110)/(200) and (b) (203) reflections for PLLA118 α′-form crystals after annealing at 150 and 160 °C for various periods (t_as). (c) t_a dependence of the content for the α-crystal ($C(\alpha)$) formed during annealing process at 150 and 160 °C. The dashed lines in (a) and (b) represent respectively the $d_{110/200}$ and d_{203} values of the normal PLLA118 α-form.

unaltered. This confirms that the PLLA sample almost does not degrade thermally under the used annealing conditions.

Results and Discussion

WAXD Patterns. Figure 1 shows the WAXD patterns of PLLA118 α′-crystals after annealing at 150 °C for different periods (t_a = 0−1440 min). The zoomed-up profiles for the weaker reflections are depicted in Figure 1b. The WAXD profile of normal PLLA118 α-crystal, which was developed by melt-crystallization at 150 °C for 12 h, is also presented in Figure 1 for comparison. Indexing of the observed reflections is based on the crystalline structure reported for the α-crystal by Miyata and Masuko.[12c] Several major features should be addressed for Figure 1. First, as t_a increasing, the two strongest reflections, that is, (110)/(200) and (203), as well as the (018) reflection shifts to the higher 2θ side. Second, the (004)/(103) and (204) reflections, which are almost absent in the α′-crystal, are present with annealing. Third, as for the (010) and (015) reflections, their intensities increase gradually with increasing t_a. Because of the more ordered and compact structure of the α-crystal, it has been reported that the (110)/(200) and (203) reflections of the α-crystal show at higher 2θ, and also more reflections are present, when compared to the α′-crystal.

Furthermore, only one reflection (indicated by the arrow in Figure 1b), which is the characteristic diffraction of the α′-crystal,[5a] can be detected at nearby $2\theta = 24.5°$ in the unannealed α′-crystal. However, as t_a is increased, two peaks, corresponding to (206) and (016) reflections of the PLLA α-crystal,[12c] are observed in this region. In a word, with increasing t_a, many diffraction features relating to the α-crystal are present in the WAXD patterns. After annealing at 150 °C for 1440 min, except for the relative intensities of some peaks, the WAXD profile is almost the same as that of the normal α-crystal, as shown in Figure 1. These strongly suggest that the α′-crystal transforms into the α one during annealing at the elevated temperature. On the other hand, the variation tendency of the characteristic reflections ($2\theta \approx 24.5°$) for the α′-crystal is of interest. As seen in Figure 1b, it first shifts to higher 2θ side when $t_a < 360$ min, and then a weak peak, that is, (016) reflection of the α-crystal, is present in its lower 2θ side. These indicate that the peak presented at nearby 24.5° in the WAXD profile of the α′-crystal is ascribed to the (206) reflection.

In order to illustrate the variation of crystalline structure during the annealing process, the lattice spacings (d) of the (110)/(200) and (203) diffractions, $d_{110/200}$ and d_{203}, were evaluated by the Bragg equation on the basis of the results shown in Figure 1. The values of $d_{110/200}$ and d_{203} are respectively plotted as a function of t_a in parts a and b of Figure 2, where the d values of the normal α-crystal are also indicated by the dashed lines. Since the α′-form possesses a disordered and looser structure related to the chain packing manner and conformation,[5] it is obvious that the α′-to-α transition of PLLA is a disorder-to-order transformation. During the phase transition, the chain packing in the unit cell becomes more compact. Therefore, with increasing t_a, both the values of $d_{110/200}$ and d_{203} reduce, as shown in Figures 2a,b. This signifies that the unit cell dimension decreases in the annealing process. When t_a reaches 1440 min, the $d_{110/200}$ and d_{203} values are almost the same to those of the normal α-crystal, suggesting most of the α′-crystals have been transformed into the α ones.

Before the α′-crystals completely transform into the α-crystals, the system is a mixture of the α′- and α-crystals. Therefore, the lattice spacings shown in Figures 2a,b are the average values of the α′- and α-crystals. Assuming that the lattice spacing varies linearly with the content of the α-phase formed during the annealing process, the content of the α-phase in the mixture system, symbolized as $C(\alpha)$, can be estimated as follows:

$$C(a) = \frac{d_{ldk}(\alpha') - d_{ldk}(T_a, t_a)}{d_{ldk}(\alpha') - d_{ldk}(\alpha)} \quad (1)$$

where $d_{ldk}(\alpha')$ and $d_{ldk}(\alpha)$ represent the lattice spacings derived from the (ldk) diffraction for the unannealed α′-crystal and the normal α-crystal, respectively. $d_{ldk}(T_a,t_a)$ is the lattice spacing of the system after annealing at T_a for t_a. Here, the strongest reflection, that is, (110)/(200), was used to estimate $C(\alpha)$. The evaluated $C(\alpha)$ for the PLLA118 α′-crystal after annealing at 150 °C is shown in Figure 2c as a function of t_a.

In addition, the annealing experiment for the PLLA118 α′-crystal at 160 °C was also performed. On the basis of the original WAXD profiles, the $d_{110/200}$, d_{203}, and $C(\alpha)$ values were evaluated and are plotted as a function of t_a in parts a, b, and c of Figure 2, respectively. At T_a = 150 °C, the $d_{110/200}$ and d_{203} values decrease, and the $C(\alpha)$ value increases gradually with the increase of t_a. However, when T_a is increased to 160 °C, the decreases of $d_{110/200}$ and d_{203} and the increase of $C(\alpha)$ are very rapid at the initial annealing stage ($t_a < 30$ min), and then they almost remain unchanged with further increasing of t_a ($t_a > 30$ min). Thses results indicate that for the PLLA118 α′-crystal annealed at 160 °C the phase transition is very fast, and it almost finishes within 30 min. It can be concluded that besides t_a, the T_a value also strongly affects the phase transition process. With the increase of T_a, this transition process becomes much faster.

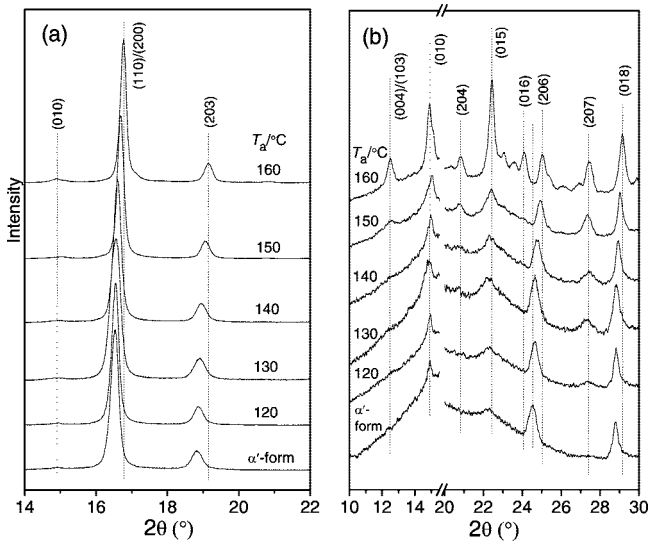

Figure 3. (a) WAXD patterns and (b) enlarged patterns of PLLA118 α′-crystals unannealed and annealed at the indicated temperatures (T_a/°C) for 360 min.

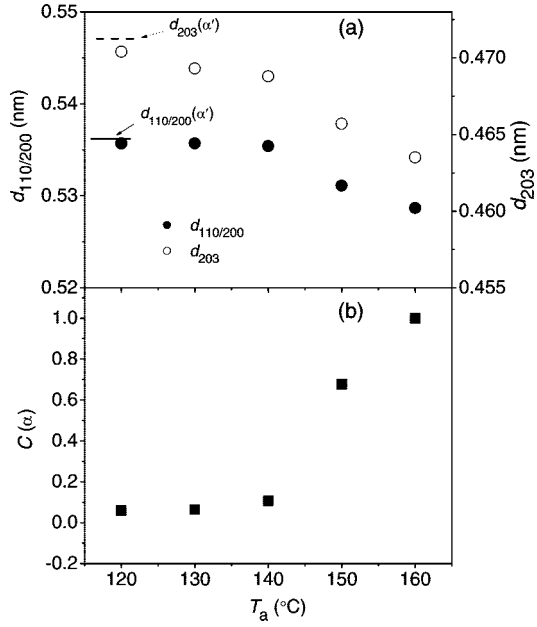

Figure 4. (a) Lattice spacings estimated from the (110)/(200) and (203) reflections in Figure 3 for the PLLA118 α′-crystals after annealing at different temperatures (T_as) for 360 min. (b) Content for the formed α-crystal ($C(\alpha)$) as a function of T_a derived from the results shown in Figure 3. The solid and dashed lines in (a) represent the $d_{110/200}$ and d_{203} values of the unannealed α′-form, respectively.

The effect of annealing temperature on the phase transition behavior was further studied by WAXD analysis. The WAXD patterns of the PLLA118 α′-crystals unannealed and annealed at different T_as for 360 min are depicted in Figure 3. On the basis of the WAXD profiles, $d_{110/200}$, d_{203}, and $C(\alpha)$ for this annealing system were estimated, which are shown as a function of T_a in Figures 4a,b. As shown in Figure 3, at the same annealing period, the diffraction features of the α-crystal in these WAXD patterns can be observed more and more clearly with increasing T_a, corresponding to the decrease in the lattice spacings and the enhancement in the content of the α-crystal (see Figure 4). Furthermore, when the T_a value is lower than 140 °C, the changes in the WAXD profiles are very small after annealing for 360 min, and only little shift of the diffraction peaks, that is, (110)/(200), (203), (206), and (018),

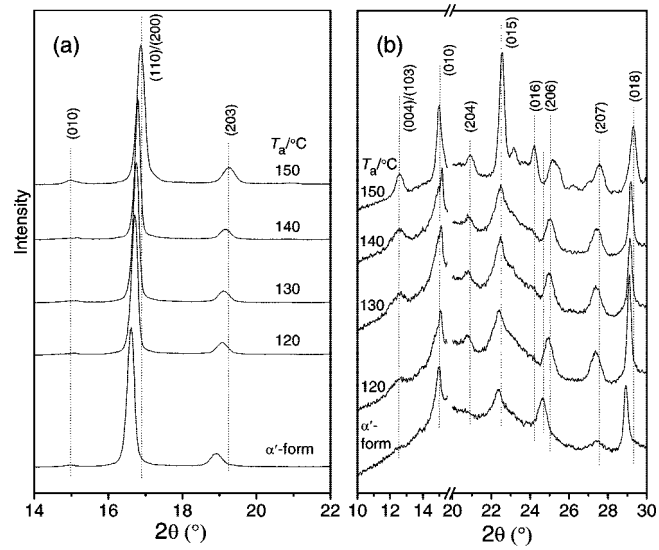

Figure 5. (a) WAXD patterns and (b) enlarged patterns of the PLLA15 α′-crystals unannealed and annealed at the indicated temperatures (T_a/°C) for 360 min.

was observed, as shown in Figure 3. As shown in Figure 4b, the estimated content of the α-phase formed during annealing process is less than 10% after annealing at T_a < 140 °C for 360 min. These results indicate that the α′-to-α transition proceeds very slowly at T_a < 140 °C. Nevertheless, as seen in Figure 3, with the increase of T_a from 140 to 150 °C, the shift of the previous WAXD peaks becomes much more prominent, corresponding to the sharp changes in $d_{110/200}$, d_{203} and $C(\alpha)$ shown in parts a and b of Figure 4. Therefore, it can be concluded that T_a plays an important role in the α′-to-α phase transition kinetics, and the polymorphic transition in PLLA118 becomes much rapider with increasing T_a to higher than 140 °C.

To study the effect of MW, the phase transition behavior of the low-MW sample (M_n = ~15K) was also investigated by WAXD analysis. As for the PLLA15 α′-crystal annealed at 140 and 150 °C, the similar changes in WAXD patterns as those of PLLA118 were observed with increasing t_a. Hence, only the results concerning the T_a effect on phase transition are shown here. Figure 5 depicts the WAXD patterns for the PLLA15 α′-crystal unannealed and annealed at different T_as for 360 min. On the basis of the profiles shown in Figure 5, $d_{110/200}$, d_{203} and $C(\alpha)$ were estimated, which are shown as a function of T_a in parts a and b of Figure 6, respectively. As compared to those of PLLA118, the annealing-induced changes in the WAXD patterns shown in Figure 5, such as the shift of (110)/(200), (203), (206), and (018) and the presence of (004)/(103) and (204) reflections, are much more distinct even when the T_a value is as low as 120 °C. As seen in Figure 6, after annealing at 120 °C for 360 min, the values of $d_{110/200}$ and d_{203} decrease considerably, and approximately half of the α′-crystals transform into the α ones. This indicates that the α′-to-α transition proceeds rapidly in the low-MW PLLA even when annealed at relatively lower temperature. Besides, with increasing T_a, the $d_{110/200}$ and d_{203} decrease, and $C(\alpha)$ increases gradually and continuously, which is different from the discrete changes of d, $C(\alpha)$ vs T_a shown in Figure 4 for PLLA118. Comparing the results shown in Figures 4b and 6b, at the identical annealing conditions (T_a, t_a), $C(\alpha)$ is much larger for PLLA15. This suggests that the α′-to-α transition process becomes more rapid with the decrease of MW. The further discussion about the MW effect on the annealing-induced phase transition behavior will be made in the following section in combination with the FTIR results.

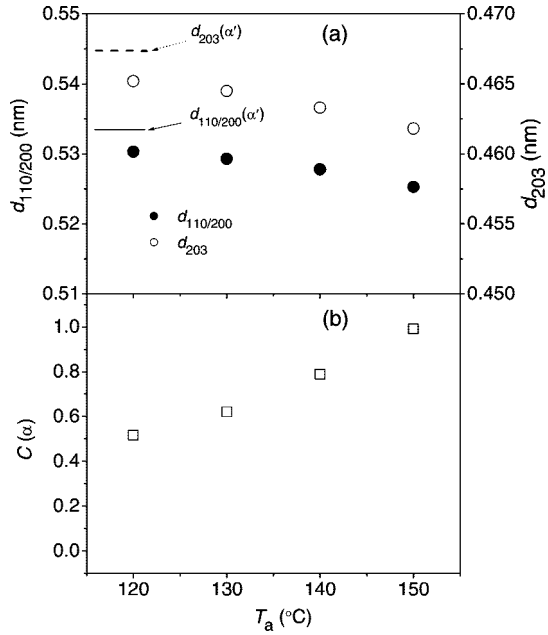

Figure 6. (a) Lattice spacings estimated from the (110)/(200) and (203) reflections for the PLLA15 α′-crystals after annealing at different temperatures (T_as) for 360 min. (b) Content of the formed α-crystal ($C(\alpha)$) as a function of T_a derived from the results shown in Figure 5. The solid and dashed lines in (a) represent the $d_{110/200}$ and d_{203} values of the unannealed PLLA15 α′-form, respectively.

FTIR Spectra. Since the PLLA α′- and α-crystals show the different FTIR spectra,[5a,b] the structural changes during annealing process could be detected by using FTIR spectroscopy. It has been reported that the carboxyl stretching (1800−1700 cm^{-1}) and 1300−1000 cm^{-1} regions are sensitive to the conformation, intra- and intermolecular interaction of PLLA chains.[13] Therefore, the spectra in these ranges will be mainly analyzed here. FTIR spectra in the 1800−1700 and 1260−1000 cm^{-1} regions for the PLLA118 α′-crystal after annealing at 150 °C for various periods are presented in Figures 7a and 8a, respectively. The spectrum of the normal PLLA118 α-crystal, which is developed by melt-crystallization at 150 °C for 12 h, is also depicted for comparison. The corresponding second derivatives are shown in part b of Figures 7 and 8. One can clearly observe the spectral difference between the α′- and α-crystal from Figure 7. Several components at about 1749, 1768, and 1777 cm^{-1} are split in the α-crystal, in which the 1749 cm^{-1} one is the most distinct. However, these splitting bands, especially the 1749 cm^{-1} one, cannot be clearly observed in the unannealed α′-crystal. As shown in Figure 7, these splitting bands become much clearer during annealing process. Especially, the intensity of the 1749 cm^{-1} band, which is the characteristic band of the PLLA α-crystal,[5a,b] enhances significantly with annealing, strongly suggesting that the α-crystal is formed during annealing process and its content increases with increasing t_a. Combined with the aforementioned WAXD results, it is further confirmed that the α′-to-α phase transition occurs during the annealing process at the elevated temperatures.

Because of the high overlapping of the stretching vibration of C−O−C bond and rocking vibration of CH_3 (and CH) bonds, very complicated spectrum is presented in 1260−1000 cm^{-1} range, as shown in Figure 8. According to Kister et al.,[13a] the observed FTIR bands for the PLLA α′- and α-crystals in this range were assigned, as tabulated in Table 2. First, we focus on the band splitting phenomena in this region. As shown in Figure 8, two clear splitting components, that is, 1053 and 1222 cm^{-1} bands, which respectively originate from ν(C−CH_3) and ν_{as}(C−O−C) + $r_{as}(CH_3)$ vibration modes, are characteristic for

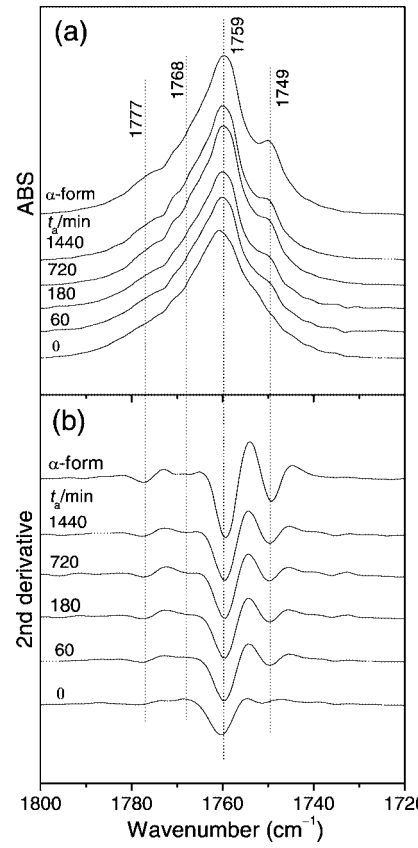

Figure 7. (a) FTIR spectra and (b) corresponding second derivatives in the frequency region 1800−1720 cm^{-1} measured for the normal PLLA118 α-crystal and annealed (at 150 °C for various periods (t_a/min)) PLLA118 α′-crystals.

the α-crystal. As seen in Figure 8b, these two bands are present in the annealed α′-crystal, and they can be observed more and more distinctly with increasing t_a. These results also support the conclusion that the α′-crystal transforms into the α one upon annealing.

As seen in Figure 8, it can be seen that the spectral features (including the spectral shape and the position of some bands) in the vibration region of ν_{as}(C−O−C) + $r_{as}(CH_3)$, that is, 1260−1160 cm^{-1}, are significantly different between the α′- and α-crystals. It was also found that the ν_{as}(C−O−C) + $r_{as}(CH_3)$ band is sensitive not only to the crystal modifications but also to the crystallization temperature (data not shown). In other words, even for the α-crystals which are developed at different crystallization temperatures, the FTIR spectra for the ν_{as}(C−O−C) + $r_{as}(CH_3)$ band are also different. The recent report of Meaurio et al.[13c] also confirms this. Because of the complexity of the fingerprint bands and the highly spectral overlapping in this region, the origin of this phenomenon is still unclear. One plausible explanation could be due to the extremely high sensitivity of the ν_{as}(C−O−C) band to the crystallinity, chain conformation, and/or chain packing manner. From a theoretical point of view, the crystallinity, chain conformation, and/or chain packing manner in PLLA crystallized at different crystallization temperatures may not be completely identical because of the dissimilar kinetics and intrinsic viscosity of the crystallization system.

Moreover, as shown in Figure 8a, it is notable that, except for the splitting at 1222 cm^{-1}, the spectral shapes as well as the relative intensity of 1213 and 1183 cm^{-1} peaks in the ν_{as}(C−O−C) + $r_{as}(CH_3)$ region change little during annealing process. This is to say, the spectral features in the 1260−1160 cm^{-1} range of the α-crystal formed in the phase transition

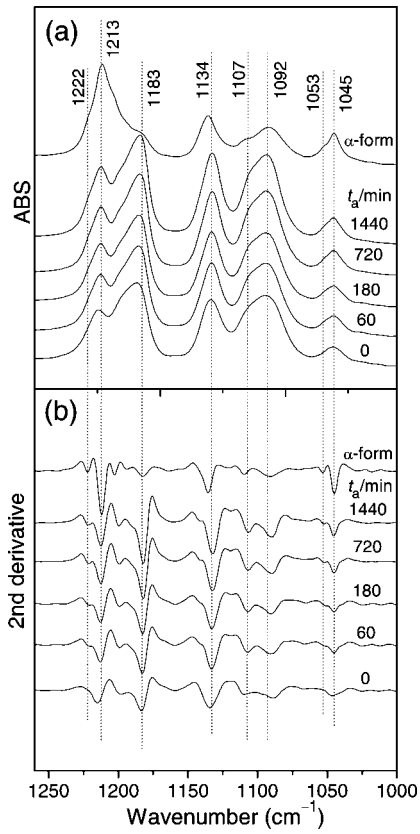

Figure 8. (a) FTIR spectra and (b) corresponding second derivatives in the frequency region 1260−1000 cm^{-1} recorded for the normal PLLA118 α-crystal and annealed (at 150 °C for various periods (t_a/min)) PLLA118 α′-crystals.

Table 2. Assignments for the FTIR Bands in the 1260−1000 cm^{-1} Region for PLLA α′- and α-Crystals

IR frequencies (cm^{-1})		
α′	α	assignments
1213	1213	ν_{as}(C−O−C) + r_{as}(CH_3)
	1222	
1183	1183	
1134	1134	r_s(CH_3)
1092	1092	ν_s(C−O−C)
1107	1107	
1045	1045	ν(C−CH_3)
	1053	

process are different from those of the normal α-form developed by the melt-crystallization at the same temperature (150 °C). This observation suggests that the structure and/or morphology of these two types of α-crystals, symbolized as α_{pt} (formed in the annealing-induced phase transition process at T_a) and α_{mc} (developed in the melt-crystallization at the same temperature as T_a), are more or less different with each other. Consequently, it is considered that the annealing-induced phase transition is not likely to be the solid−melt−solid process, which proceeds via the melt-recrystallization mechanism. If the melt-recrystallization process occurs during annealing process, the formed crystalline phase will possibly be the α_{mc}-type, which contradicts the FTIR results shown in the ν_{as}(C−O−C) + r_{as}(CH_3) region. Therefore, it is proposed that the α′-to-α transformation during annealing at elevated temperature is the direct solid−solid phase transition. This suggestion is also supported by the recent report of Kawai et al.[5c] on the melting behavior of PLLA studied using the temperature-variable WAXD method.

As shown in Figures 7 and 8, the changes in FTIR spectra upon annealing are mainly associated with the splitting of ν(C═O) and ν(C−CH_3). Besides, the splitting of the δ(CH_3) band (1500−1320 cm^{-1}) was also observed during the annealing process (data not shown). These all are related to the side groups, i.e., C═O, CH_3, and C−CH_3. Despite extensive studies on the vibration spectra of PLLA α-crystal, the origin of spectral splitting is still not well interpreted, especially for the ν(C═O) band. So far, it has been proposed that this splitting of ν(C═O) band can be attributable to the intramolecular coupling[13b] or correlation field splitting arising from the interchain interaction.[13d] The former is sensitive to the chain conformation and the distribution of conformers. The correlation field splitting, also called as factor group splitting or Davydov splitting,[16] occurs due to the lateral interaction between the chains contained in the unit cell, splitting the absorption in a number of components. In the case of orthorhombic unit cell of PLLA, the transition moments of the two adjacent PLLA chains can couple in phase or out of phase, leading to the splitting in the FTIR absorption.[13c]

At present, it has been known that the chain conformation and packing between the α′- and α-crystals are different slightly.[5] Therefore, it is considered that the PLLA chains will readjust to the more stable and energy-favorable conformation and packing manner within the unit cell, during the annealing-induced phase transition process. As far as the chain packing is concerned, its rearrangement from the looser to more compact state during the phase transition decreases the intermolecular distance, accompanied by the reduction of unit cell volume. Shorter intermolecular distances usually translate into enhancement of interactions, resulting in the presence of many splitting bands during the annealing-induced phase transition process.

On the other hand, the slight readjustment of the chain conformation can also possibly induce the change of FTIR spectra because of its effect on the intramolecular interaction. For further discussion, the groups in the PLLA chain are considered as two parts, i.e., the C−O−C backbone and the side groups (C═O, CH_3). As mentioned above, the spectral splitting observed during the phase transition process is mainly related to the side groups, and relatively small spectral change is detected in the band related to the C−O−C backbone, for example, the ν_{as}(C−O−C) + r_{as}(CH_3) band. This might suggest that the slight difference between the chain conformation of PLLA α′- and α-crystals is mainly related to the side groups. It is considered that during the annealing-induced α′-to-α transition process the readjustment of the chain conformation and lateral packing manner occur simultaneously.

The influence of annealing temperature and MW on the phase transition behavior was also investigated by FTIR. Parts a and b of Figure 9 show the FTIR spectra in the carbonyl stretching region for the high-MW (PLLA118) and low-MW (PLLA15) samples annealed at different T_as for 360 min, respectively. As for the PLLA samples annealed for the same period, the splitting bands, especially the one at 1749 cm^{-1}, become much more distinct with increasing T_a, accompanied by the increase of the intensity, as shown in Figure 9. As concerning PLLA118, when the T_a value is below 140 °C, the change of the 1749 cm^{-1} band is so small that it cannot be clearly discerned after annealing for 360 min. At T_a > 140 °C, the annealing-induced increase in the intensity of the 1749 cm^{-1} band becomes much distinct. These results further indicate that the α′-to-α transition proceeds much more prominently when annealed at above 140 °C. However, in the case of PLLA15, the increase in the intensity of 1749 cm^{-1} band can be distinctly detected even after annealing at 120 °C, suggesting that the α′-crystal transforms into the α one evidently in this annealing process. All these results are well consistent with the above-mentioned WAXD data.

The MW effect on the phase transition can be explained by the mobility of polymer chains. The equilibrium melting point

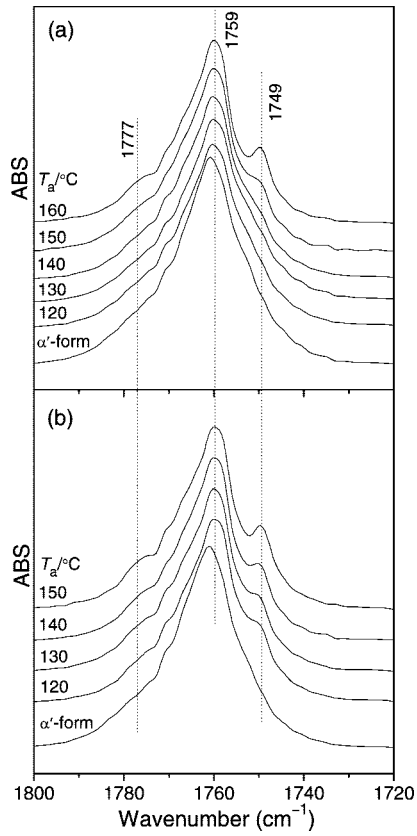

Figure 9. FTIR spectra in the 1800−1720 cm^{-1} region for the unannealed and annealed (at the indicated temperatures (T_a/°C) for 360 min) α′-crystals of (a) PLLA118 and (b) PLLA15.

(T_m^0) of PLLA15 is about 20 °C lower than that of PLLA118, as shown in Table 1. When annealed at the same temperature, the chains of PLLA15 possess a higher mobility because of the smaller undercooling ($T_m^0 - T_a$) and intrinsic viscosity. Accordingly, the rearrangement of the chain conformation and packing in PLLA15 is easier and faster during the annealing process. Therefore, the α′-to-α transition is more rapid in the low-MW PLLA, and it proceeds prominently even when annealed at relatively lower T_a.

DSC Melting Behavior. It has been reported that the PLLA α′- and α-crystals show different melting behavior upon heating.[5a,c,d] Consequently, study on the melting behavior of the annealed α′-form can probably reflect the structural and morphological changes during the phase transition. Figures 10a,b show the DSC melting curves for the PLLA118 and PLLA15 α′-crystals annealed at 140 °C for different t_as. Obviously, the melting behavior of PLLA α′-crystal changes considerably after the annealing process. As depicted in Figure 10a, as for the unannealed PLLA118 α′-crystals, an exotherm (P_{exo}) arising from the α′-to-α transition upon heating can be observed prior to the major melting peak (P_1).[5a,c,d] After annealing at T_a for a relatively short period, some α′-crystals transform into the α ones, and the system is a mixture of the initial α′-crystal and α-crystal formed in the annealing process. During the following heating scan, two processes, that is, (i) the α′-to-α transition (occurring upon heating) and (ii) melt-recrystallization of the α-crystal formed in the previous annealing process, take place synchronously before the final melting (P_1). From a theoretical viewpoint, processes i and ii are generally exothermic and endothermic processes, respectively.

For PLLA118 annealed for a shorter periods (t_a = 10−120 min), only relatively small amount of α′-crystal transforms into the α one. In the heating scan, the contributions of processes i and ii severely overlap, resulting in the quite broad peak (P_2)

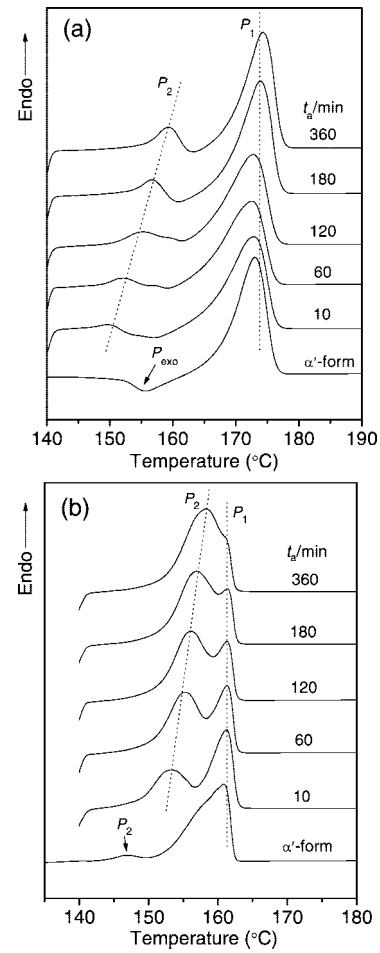

Figure 10. DSC thermographs recorded in the heating scan at 10 °C/min for the (a) PLLA118 and (b) PLLA15 α′-crystals unannealed and annealed at 140 °C for the indicated periods (t_a/min).

observed at 145−160 °C, as shown in Figure 10a. With the further increase of t_a, the α-crystal content increases, and the contribution of process ii enhances. So, a clear endotherm (P_2) is present before the dominant melting peak (P_1) during the heating scan of PLLA118 α′-crystal annealed for $t_a \geq 180$ min. With increasing t_a, the endotherm P_2 shifts to the higher temperature and increases in its magnitude. According to the report concerning the β-to-α transition in poly(butylene adipate) by Gan et al.,[14] it is considered that the thickening and perfecting of the lamellar crystals of the original α′-crystal and the α-crystal formed during the annealing process also possibly occur upon annealing.

As reported previously,[5a] the α′-crystal of low-MW PLLA shows a more complicated melting behavior upon heating scan (see Figure 10b) than that of the high-MW sample. Here, we mainly focus on the effects of t_a and T_a on the melting behavior. For the PLLA15 sample annealed at 140 °C for only 10 min, the endotherm (P_2) prior to the final melting peak (P_1) can be clearly observed upon the heating scan. With the further increase of t_a, the P_2 peak increases in magnitude and also shifts to higher temperature gradually. The endotherm P_2 almost merges with the P_1 peak after annealing for 360 min. These indicate that the contribution of process ii, that is, the melt-recrystallization of the α-crystal formed during the annealing process, becomes more and more dominant with the gradual increase of the α-crystal content during annealing. For the annealed PLLA118 and PLLA15 samples, the major endotherm P_1 shown in Figure 10 is ascribed to the final melting of the α-crystal formed in the (I) α′-to-α phase transition (upon heating) and (II) melt-crystallization processes. Therefore, the peak temperature of

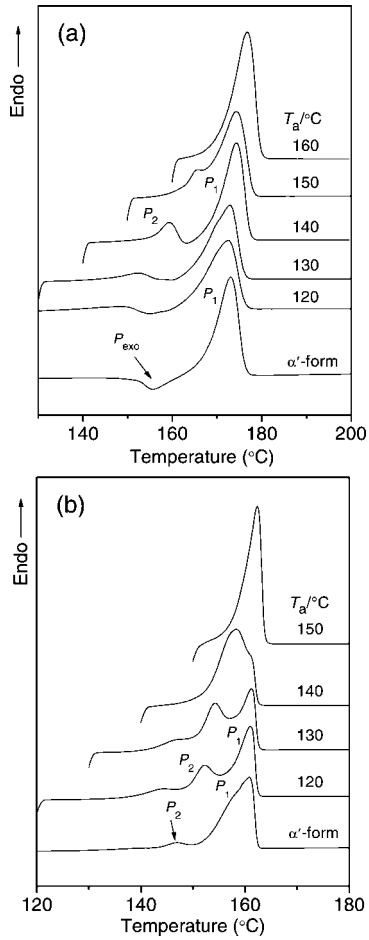

Figure 11. DSC thermographs recorded in the heating scan at 10 °C/min for the (a) PLLA118 and (b) PLLA15 α′-crystals unannealed and annealed at the indicated temperatures (T_a/°C) for 360 min.

endotherm P_1 is almost unchanged with increasing t_a. The contrast between the results shown in Figures 10a,b also suggests that when annealed at the same T_a, the α′-to-α transition become faster with the decrease of MW.

The effects of annealing temperature on the subsequent melting behavior of PLLA118 and PLLA15 are shown in parts a and b of Figure 11, respectively. As for PLLA118, the annealing-induced change in the DSC heating curves is relatively smaller when annealed at $T_a < 140$ °C for 360 min, as presented in Figure 11a. However, in the case of PLLA15, distinct changes in the melting behavior can be detected when annealed at $T_a = 120$ °C. These are in well agreement with the WAXD and FTIR results and further demonstrate that the α′-to-α transition is rapid and also can proceed prominently in the low-MW PLLA even when annealed at relatively lower T_a. As seen in Figure 11, only one endotherm is observed in the samples annealed at very high T_a (160 °C for PLLA118 and 150 °C for PLLA15) because of the complete transformation from the α′- to α-crystal.

Conclusion

In the present report, the effects of annealing period, temperature, and MW on the crystalline phase transition in the PLLA α′-crystal were investigated by WAXD, FTIR, and DSC. Both the WAXD and FTIR results clearly indicate that the α′-to-α transition occurs during the annealing process at the elevated temperature. It was found that both t_a and T_a play the important roles in the phase transition process. As increasing T_a, the phase transition process proceeds more rapidly. During the α′-to-α transition process, the unit cell dimension reduces. The mechanism for the α′-to-α transformation was proposed to be the solid−solid transition process, which involves the readjustment of the chain conformation (especially related to the side groups) and packing manner in the unit cell to more energy-favorable state. DSC melting behavior indicates that the α-crystal formed during annealing process undergoes the melt-recrystallization process in the heating scan. Furthermore, it was found that the MW of PLLA affects the α′-to-α transition greatly. In the low-MW PLLA, the α′-to-α transition becomes much more rapid and can proceed prominently even when annealed at relatively lower T_a. Through this study, the phase behavior as well as the structure of PLLA α′- and α-crystals can be better understood, which is thought to be useful for controlling the physical properties of PLLA-based material by regulating the crystallization and annealing processes.

Acknowledgment. The authors thank Prof. Minoru Sakurai for the use of FTIR instrument and also thank Dr. Kazue Ueda of Unitika Co. Ltd. (Kyoto, Japan) for kindly supplying PLLA samples.

References and Notes

(1) (a) Darder, M.; Aranda, P.; Ruiz-Hitzky, E. *Adv. Mater.* **2007**, *19*, 1. (b) Nair, L. S.; Laurencin, C. T. *Prog. Polym. Sci.* **2007**, *32*, 762.

(2) (a) De Santis, P.; Kovacs, J. *Biopolymers* **1968**, *6*, 299. (b) Hoogsteen, W.; Postema, A. R.; Pennings, A. J.; Ten Brinke, G.; Zugenmaier, P. *Macromolecules* **1990**, *23*, 634. (c) Kobayshi, J.; Asahi, T.; Ichiki, M.; Okikawa, A.; Suzuki, H.; Watanabe, T.; Fukada, E.; Shikinami, Y. *J. Appl. Phys.* **1995**, *77*, 2957.

(3) (a) Eling, B.; Gogolewski, S.; Pennings, A. J. *Polymer* **1982**, *23*, 1587. (b) Puiggali, J.; Ikada, Y.; Tsuji, H.; Cartier, L.; Okihara, T.; Lotz, B. *Polymer* **2000**, *41*, 8921. (c) Sawai, D.; Takahashi, K.; Sasashige, A.; Kanamoto, T.; Hyon, S. H. *Macromolecules* **2003**, *36*, 3601. (d) Brizzolara, D.; Cantow, H. J.; Diederichs, K.; Keller, E.; Domb, A. J. *Macromolecules* **1996**, *29*, 191.

(4) Cartier, L.; Okihara, T.; Ikada, Y.; Tsuji, H.; Puiggali, J.; Lotz, B. *Polymer* **2000**, *41*, 8909.

(5) (a) Pan, P.; Kai, W.; Zhu, B.; Dong, T.; Inoue, Y. *Macromolecules* **2007**, *40*, 6898. (b) Zhang, J.; Duan, Y.; Sato, H.; Tsuji, H.; Noda, I.; Yan, S.; Ozaki, Y. *Macromolecules* **2005**, *38*, 8012. (c) Kawai, T.; Rahman, N.; Matsuba, G.; Nishida, K.; Kanaya, T.; Nakano, M.; Okamoto, H.; Kawada, J.; Usuki, A.; Honma, N.; Nakajima, K.; Matsuda, M. *Macromolecules* **2007**, *40*, 9463. (d) Zhang, J.; Tashiro, K.; Tsuji, H.; Domb, A. J. *Macromolecules* **2008**, *41*, 1352. (e) Zhang, J.; Tashiro, K.; Domb, A. J.; Tsuji, H. *Macromol. Symp.* **2006**, *242*, 274.

(6) (a) Kristiansen, M.; Tervoort, T.; Smith, P.; Goossens, H. *Macromolecules* **2005**, *38*, 10461. (b) Libster, D.; Aserin, A.; Garti, N. *Polym. Adv. Technol.* **2007**, *18*, 685.

(7) Furuhashi, Y.; Iwata, T.; Kimura, Y.; Doi, Y. *Macromol. Biosci.* **2003**, *3*, 462.

(8) (a) Auriemma, F.; De Rosa, E.; Esposito, S.; Mitchell, G. R. *Angew. Chem., Int. Ed.* **2007**, *46*, 1. (b) Yamamoto, Y.; Inoue, Y.; Onai, T.; Doshu, C.; Takahashi, H.; Uehara, H. *Macromolecules* **2007**, *40*, 2745. (c) De Rosa, C.; Ruiz de Ballesteros, O.; Auriemma, F.; Savarese, R. *Macromolecules* **2005**, *38*, 4791. (d) Guadagno, L.; Naddeo, C.; Vittoria, V.; Meille, S. V. *Macromolecules* **2005**, *38*, 8755.

(9) (a) Sun, Y. S.; Woo, E. M.; Wu, M. C.; Ho, R. M. *Macromolecules* **2003**, *36*, 8415. (b) Wang, C.; Lin, C. C.; Chu, C. P. *Macromolecules* **2006**, *39*, 9267. (c) Gowd, E. B.; Shibayama, N.; Tashiro, K. *Macromolecules* **2006**, *39*, 8412.

(10) (a) Rueda, D. R.; García Gutiérrez, M. C.; Ania, F.; Zolotukhin, M. G.; Baltá Calleja, F. J. *Macromolecules* **1998**, *31*, 8201. (b) Kawakami, D.; Hsiao, B. S.; Burger, C.; Ran, S.; Avila-Orta, C.; Sics, I.; Kikutani, T.; Jacob, K. I.; Chu, B. *Macromolecules* **2005**, *38*, 91. (c) Azzurri, F.; Alfonso, G. C.; Gómez, M. A.; Martì, M. C.; Ellis, G.; Marco, C. *Macromolecules* **2004**, *37*, 3755. (d) Molenberg, A.; Möller, M. *Macromolecules* **1997**, *30*, 8332. (e) Maeda, Y.; Osada, K.; Watanabe, J. *Macromolecules* **2000**, *33*, 2456. (f) Cheng, S. Z. D.; Cao, M. Y.; Wunderlich, B. *Macromolecules* **1986**, *19*, 1868.

(11) (a) Abe, H.; Kikkawa, Y.; Inoue, Y.; Doi, Y. *Biomacromolecules* **2001**, *2*, 1007. (b) Di Lorenzo, M. L. *Eur. Polym. J.* **2005**, *41*, 569. (c) Yasuniwa, M.; Tsubakihara, S.; Iura, K.; Ono, Y.; Dan, Y.; Takahashi, K. *Polymer* **2006**, *47*, 7554. (d) Tsuji, H.; Miyase, T.; Tezuka, Y.; Saha, S. K. *Biomacromolecules* **2005**, *6*, 244. (e) Wang, Y.; Mano, J. F. *Eur. Polym. J.* **2005**, *41*, 2335.

(12) (a) Krikorian, V.; Pochan, D. J. *Macromolecules* **2005**, *38*, 6520. (b) Krikorian, V.; Pochan, D. J. *Macromolecules* **2004**, *37*, 6480. (c) Miyata, T.; Masuko, T. *Polymer* **1997**, *38*, 4003. (d) Cho, T. Y.; Strobl, G. *Polymer* **2006**, *47*, 1036.
(13) (a) Kister, G.; Cassanas, G.; Vert, M. *Polymer* **1998**, *39*, 267. (b) Meaurio, E.; Zuza, E.; López-Rodríguez, N.; Sarasua, J. R. *J. Phys. Chem. B* **2006**, *110*, 5790. (c) Meaurio, E.; López-Rodríguez, N.; Sarasua, J. R. *Macromolecules* **2006**, *39*, 9291. (d) Aou, K.; Hsu, S. L. *Macromolecules* **2006**, *39*, 3337.
(14) Gan, Z. H.; Kuwabara, K.; Abe, H.; Iwata, T.; Doi, Y. *Biomacromolecules* **2004**, *5*, 371.
(15) (a) Medellín-Rodríguez, F. J.; Larios-Lopez, L.; Zapata-Espinoza, A.; Davalos-Montoya, O.; Phillips, P. J.; Lin, J. S. *Macromolecules* **2004**, *37*, 1799. (b) Meille, S. V.; Romita, V.; Caronna, T.; Lovinger, A. J.; Catellani, M.; Belobrzeckaja, L. *Macromolecules* **1997**, *30*, 7898. (c) Alamo, R. G.; Kim, M. H.; Galante, M. J.; Isasi, J. R.; Mandelkern, L. *Macromolecules* **1999**, *32*, 4050. (d) Acierno, S.; Grizuti, N.; Winter, H. H. *Macromolecules* **2002**, *35*, 5043. (e) Zhu, B.; He, Y.; Asakawa, N.; Nishida, H.; Inoue, Y. *Macromolecules* **2006**, *39*, 194.
(16) Lagaron, J. M. *Macromol. Symp.* **2002**, *184*, 19.

MA800343G